Analysis of the approximations applied in the continuum-distorted-wave–eikonal-initial-state theory for the evaluation of ionization cross sections: Post-prior discrepancy, axial symmetry, and ion-ion interaction

S. D. López,[1] M. Fiori,[2] and C. R. Garibotti[1]

[1]*CONICET and Centro Atómico Bariloche, 8400 S.C. de Bariloche, Argentina*
[2]*Departamento de Física, Universidad Nacional de Salta, 4400 Salta, Argentina*

When the continuum distorted wave with eikonal initial state (CDW-EIS) [D. S. Crothers and J. F. McCann, J. Phys B **16**, 3229 (1983)] theory is applied to the evaluation of ionization cross sections, many additional approximations are assumed. However, usually, the influence of these approximations is not clear. Aiming to estimate them, we compare the differential and total cross sections obtained with diverse approximations for ionization of He atoms by proton impact. We analyze the post-prior discrepancy, which depends on the perturbative Hamiltonian applied in the scattering amplitude. We study the dependence of the cross sections on the description of the initial and final states. For this purpose, we use the 1Z and 5Z variational and numerical Optimized Potential Model (OPM) [J. D. Talman, Comput. Phys. Commun. **54**, 85 (1989)] bound states for the initial target state, and for the final target state we set Coulomb waves with proper effective charges or the continuum state of an OPM potential model. The cross sections resulting from OPM post and prior versions are identical and show excellent agreement with experimental data in each case. Nevertheless, the cross section derived by the prior CDW-EIS, 5Z initial wave, and corresponding continuum state gives comparable results, requiring shorter computational work. Then we study the determination of the impact parameter ionization probability from the transition amplitudes, also including an axial symmetry for the ionization process. The hypothesis of this axial symmetry saves an angular integration in the evaluation of the probabilities. We analyze the variation of these probabilities within the post and prior formalisms and mention initial and final states, according to the supposed symmetry. We found that the probabilities derived with the axial symmetry concentrate at a lower impact parameter than the usual ones and are quite sensitive to the approximations used for the CDW-EIS evaluation. Furthermore, these probabilities underestimate distant collisions. In the last section we introduce the projectile-residual ion potential, and we discuss the effect of the diverse approximations on the dependence of the cross section as a function of the projectile scattering angle. We compare the projectile angular distribution resulting from a full Coulomb interaction between the ions with the one obtained by a screened potential, but in the latter case the theoretical distributions underestimate the experimental data. The OPM and 5Z functions give a good description of the experimental data.

PACS number(s): 34.50.Fa, 34.10.+x

I. INTRODUCTION

The continuum distorted wave with eikonal distortion initial-state method (CDW-EIS) is the most extensively used approximation for describing atomic ionization by ionic impact at medium and high energies [1–6]. It generally gives good descriptions of experimental single-ionization cross sections, but the degree of accuracy depends on additional approximations performed in the evaluation of the CDW-EIS scattering amplitude.

The first question is whether the post or the prior version of the CDW-EIS approach should be applied. The transition amplitude is the matrix element of the perturbation Hamiltonian evaluated between the EIS initial and a two-center Coulomb continuum final state. In the post formalism the perturbation Hamiltonian corresponds to the final state, while in the prior version it is derived from the initial state. For a colliding system that contains only three particles, the prior and post amplitudes are identical when the initial and final states are eigenstates of the same Hamiltonian, as in proton-hydrogen collisions. For many electron target or dressed projectiles the post-prior discrepancy depends on the procedure applied to describe the atomic states. These two versions were compared

using hydrogenic initial and final atomic wave functions for ionization of He atoms by highly charged projectiles. It was found that the prior and post versions are very sensitive to the choice of the initial or final state, respectively [7]. Recently the fully differential cross sections (FDCSs) for single ionization of helium by heavy-ion impact was evaluated using the two versions [8]. The results showed that the prior version gives a somewhat better agreement with experiments than the post amplitude. However, this conclusion remains limited to a few angular distributions of the emitted electron energies and projectile momentum transfer fixed. Here we consider double-differential and total cross sections (TCSs), which are obtained by integration over angular and energy variables; they provide mean values and seem to be more reliable than the FDCS for theoretical comparisons.

The CDW-EIS transition matrix can be given in closed analytical form when Roothan-Hartree-Fock initial states and pure Coulomb waves are used for the final three-body state. We recall that there are many works discussing the dependence of the theoretical cross sections provided by the CDW-EIS approximation on the description of the initial bound state [9,10]. Numerical wave functions resulting from solving the target Schrödinger equation with model potentials

provide the most reliable descriptions of the cross sections, but they require computational time-consuming numerical integrations [2–4,11]. A mean potential between the active and the passive electrons was introduced as an alternative to solve the target wave equation, and with this potential the post-prior discrepancies are almost eliminated [12]. TCSs are the most frequently used magnitudes in applications, but they require long computational times, and therefore, it would be convenient to determine a simpler evaluation procedure that provides these quantities with an appropriate level of accuracy.

In the independent particle model the probability of direct multiple ionization of N electrons is calculated by a binomial distribution of products of the single-ionization probabilities, considered as function of the projectile impact parameter ρ. These probabilities can be evaluated from the transition matrix, which is a function of the emitted electron momentum and the projectile momentum transfer. This requires a Fourier transform, which is usually simplified as a Bessel transform by assuming an axial symmetry, which simplifies the calculation somewhat [11,13,14]. However, it has been shown that this simplification leads to differences in the electron ejection probability and in the double-ionization cross sections [4]. We analyzed the differences of the probabilities resulting from the post and prior amplitudes, considering also the cross-effects of the approximation in the Fourier transform. Furthermore, the amplitude as a function of the impact parameter is a more appropriate magnitude for the introduction of the internuclear interaction in the evaluation of the cross sections.

In the impact parameter method the evaluation of the electron emission cross section usually neglects the internuclear interaction and the contribution to the transition amplitude is an irrelevant complex phase [15]. However, the internuclear interaction must be included when the projectile scattering is investigated, namely, when the ejected electron distribution is studied for a fixed projectile scattering angle or as a function of the momentum transferred by the projectile [6]. These cross sections were obtained in recent experimental data from kinematically complete measurements [16–18]. Most of the calculations performed up to now simulate the interaction between the projectile and the residual ion by a Coulomb potential with an effective nuclear charge. Here we also introduce an alternative description obtained by describing that interaction by a screened potential.

The aim of this paper is to analyze the cross influence of the mentioned approximations introduced in the calculation of the cross sections with the CDW-EIS method, confronting the corresponding theoretical results with measurements. We will consider proton-helium ionizing collisions. Atomic units are used except where otherwise stated.

II. THE POST-PRIOR DISCREPANCY

For the CDW-EIS approximation the initial wave function is

$$\chi_i(\mathbf{r}_{T1},\mathbf{r}_{T2},\mathbf{r}_{P1}) = \phi(\mathbf{r}_{T1},\mathbf{r}_{T2})E_{-\mathbf{v}}(\mathbf{r}_{P1})e^{i\mathbf{K}_i\cdot\mathbf{R}_{PT}}. \quad (1)$$

Here $\mathbf{r}_{jT}$ and $\mathbf{r}_{jP}$ are the relative coordinates between electron j and the target or projectile, respectively, $\mathbf{R}_{PT}$ is the relative coordinate between the heavy particles, $\mathbf{K}_i$ and $\mathbf{v}$ are the

momentum and velocity of the incident projectile, $\mathbf{K}_f$ is the final momenta of the projectile, and $\mathbf{k}_1$ is the momentum of the emitted electron. When using a central potential model or Hartree-Fock or Configuration Interaction expansions, the initial atomic state is given by a linear superposition of terms separable in the electrons coordinates, with the form

$$\phi(\mathbf{r}_{T1},\mathbf{r}_{T2}) = \phi_a(\mathbf{r}_{T1})\phi_b(\mathbf{r}_{T2})$$

and

$$E_{-\mathbf{v}(\mathbf{r}_{P1})} = e^{i\frac{Z_P}{V}\ln(vr_{P1}+\mathbf{v}\cdot\mathbf{r}_{P1})}.$$

This wave function is an eigenfunction of the three-body Hamiltonian when the perturbation Hamiltonian is

$$H_I^i = -\tfrac{1}{2}\nabla_{r_{P1}}^2 + \boldsymbol{\nabla}_{r_{P1}}\cdot\boldsymbol{\nabla}_{r_{T1}}.$$

The final state is written as a C2 function, which approximates the more complete C3 function [19], which also considers the internuclear interaction. The C2 wave is given by

$$\chi_f(\mathbf{r}_{T1},\mathbf{r}_{T2},\mathbf{r}_{P1},\mathbf{r}_{P2}) = \psi_{\mathbf{k}_1}(\mathbf{r}_{T1})D_{\mathbf{k}_1-\mathbf{v}}(\mathbf{r}_{P1})e^{i\mathbf{K}_f\cdot\mathbf{R}_{PT}}. \quad (2)$$

Here

$$\psi_{\mathbf{k}}^{\pm}(\mathbf{r}) = e^{i\mathbf{k}\cdot\mathbf{r}}D_{\mathbf{k}}(\mp in, 1, \pm i(kr \mp \mathbf{k}\cdot\mathbf{r}))$$
$$= \Gamma(1 \pm in)e^{-\frac{n\pi}{2}}e^{i\mathbf{k}\cdot\mathbf{r}}F_{11}\left(\mp in, 1, \pm \frac{i}{\hbar}(kr \mp \mathbf{k}\cdot\mathbf{r})\right),$$

with $n = Z/k$, and Z is the charge of the heavy particle. In this case the perturbation Hamiltonian is

$$H_I^f = \boldsymbol{\nabla}_{r_{P1}}\cdot\boldsymbol{\nabla}_{r_{T1}}.$$

The transition matrix is

$$T_{fi} = \langle \chi_f^- |W| \chi_i^+ \rangle,$$

where $W = H_I^i$ for the prior approximation and $W = H_I^{f\dagger}$ for the post one. Possible dependence on the electron-electron coordinate $\mathbf{r}_{12} = \mathbf{r}_{T1} - \mathbf{r}_{T2}$ could be introduced when variational initial atomic states or the Coulombian correlation in the final state are used [20].

The fully differential cross section is

$$\frac{d\sigma}{d\mathbf{k}_1 d\mathbf{K}_f} = (2\pi)^4\frac{\mu}{K_i}|T_{fi}|^2\delta\left(\frac{K_i^2}{2\mu} + \varepsilon_i - \frac{K_f^2}{2\mu} - \frac{k_1^2}{2}\right). \quad (3)$$

Here μ is the reduced mass projectile-target and ε_i is the ionization energy of the target. Integration on the momentum of the projectile gives the double-differential cross section:

$$\frac{d\sigma}{d\mathbf{k}_1} = (2\pi)^4\mu^2\frac{K_f}{K_i}\int|T_{fi}|^2 d\Omega_{K_f},$$
$$\frac{d\sigma}{dEd\Omega_e} = (2\pi)^4\mu^2\frac{k_1 K_f}{K_i}\int|T_{fi}|^2 d\Omega_{K_f}.$$

Further integrations lead to the simple differentials, in energy or angle, and TCSs.

In Figs. 1 and 2 we compare the cross section doubly differential in the angle and energy of the electron, for a fixed emission angle $\theta_e = 0°$, as a function of the energy of the electron emitted for 100 and 1500 keV protons impinging on He, respectively. We show the results obtained with the post and prior approximation and with a variational 1Z and a
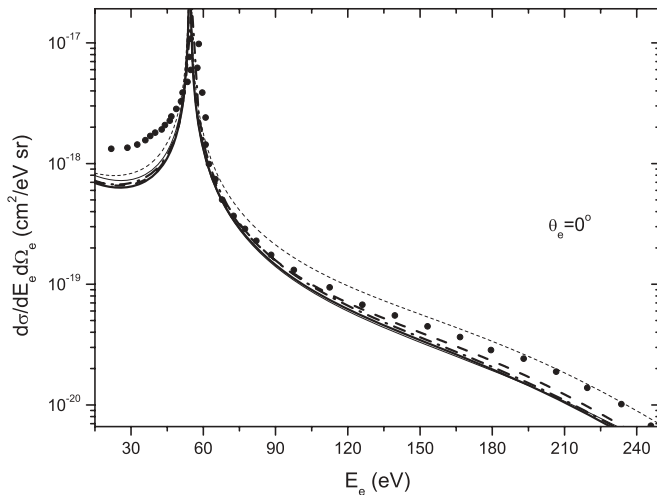
FIG. 1. Doubly differential cross section as a function of electron energy for 100 keV protons impinging on He targets. Thick(thin) curves: 5Z(1Z) initial functions. Solid lines: prior approximation. Dashed lines: post approximation. Dash-dotted lines: OPM potential. Dots: experimental data from Bernardi *et al.* [23].

Roothan-Hartree-Fock 5Z initial atomic wave function [21]. For a 1Z initial state we suppose that the final target ion has an effective charge $Z_{\text{eff}} = 1.687$, which is the variational charge of the bound state with energy 0.848 a.u. This assures the orthogonality of initial and final states. Meanwhile for the 5Z state we set $Z_{\text{eff}} = 1.345$, which results from applying the rule $Z_{\text{eff}} = \sqrt{-2\varepsilon_i}$, ε_i being the ionization energy corresponding to the 5Z model, with bound energy 0.9045 a.u. A more precise description can be given by using model potentials. In this work we have applied the optimized potential model (OPM) to evaluate the initial and final active electron target states [22]. This amounts to numerically solving the radial
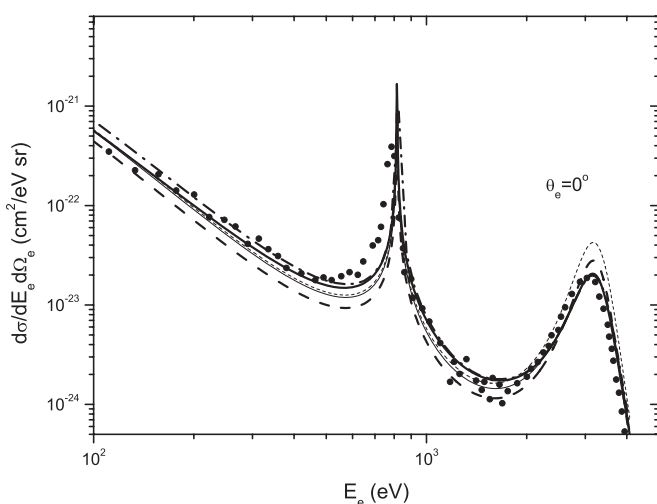

FIG. 2. Doubly differential cross section as a function of electron energy for 1500 keV protons impinging on a He target. Thick(thin) curves: 5Z(1Z) initial functions. Solid lines: prior approximation. Dashed lines: post approximation. Dash-dotted lines: numerical functions from OPM potential. Dots: experimental data from Lee *et al.* [24].

Schrödinger equation and integrating the amplitude [11]. In this case, the initial and final states are eigenstates of the same atomic potentials, and the cross sections resulting from the post and prior versions are identical. The resulting theoretical cross sections are compared to experimental data of Bernardi *et al.* [23] for 100 keV protons and those of Lee *et al.* [24] for 1500 keV protons.

All these theoretical approaches account for the capture to continuum peak that depends on the electron-projectile wave, but they are deficient in the description of their asymmetry. For an impinging energy of 100 keV, the ridge between the electron capture into the continuum (ECC) and the soft peaks is underestimated, whereas it is better described for a 1500 keV collision; this clearly shows that the CDW-EIS approach improves at high impact energies. This indicates that in the CDW-EIS the interaction between projectile and electron is somewhat weak and should be enforced, so as to increase the probability of finding the electron in the potential saddle between the ions. A larger spatial proba-bility in this region suggests a higher cross section in the energy ridge. The depth of this saddle should decrease as the projectile velocity increases, and this mechanism could justify the better agreement observed for the 1500 keV case. Gulyás and Fainstein [25] show that the description of the ridge at intermediate energies can be improved by replacing the EIS approximation in the projectile-electron wave function with a full Coulomb distortion. A mathematical comparison clearly shows that a hypergeometric function is more concentrated at small distances than an eikonal wave.

The cross section obtained with the prior version and 5Z initial state agree quite well with the OPM results and gives a better description of the experimental data than the other approaches. In the prior version the perturbation potentials, which are differential operators within the CDW–EIS approximation, operate on the initial state, while in the post version they operate on the final state.

The differential nature of the perturbation potentials makes the prior(post) version more sensitive to the quality of the initial(final) states, on which they respectively operate. This has been demonstrated by using hydrogenic initial bound and final continuum wave functions with effective charges for proton-He ionizing collisions and varying these charges [7]. In particular, in the post version it may be possible to change the final effective charge to make it closer to the prior version, without the introduction of a mean potential [12]

The 5Z wave function for the initial bound state that we are using here can be regarded as a very good one, but the same cannot be stated for the final continuum state with an effective charge. The angular distributions evaluated with a prior amplitude, with the 5Z initial state, depend slightly on changes in the final effective charge. Therefore use of the prior version is a more accurate procedure for application of the CDW-EIS formalism. Furthermore, we should note that for atomic targets precise bound states are currently available, but finding accurate effective charges for the final continuum state remains a speculative problem.

The deviations between prior and post versions are more significant for highly charged projectiles, because they are determined by the Sommerfeld parameter Z_P/v [7].
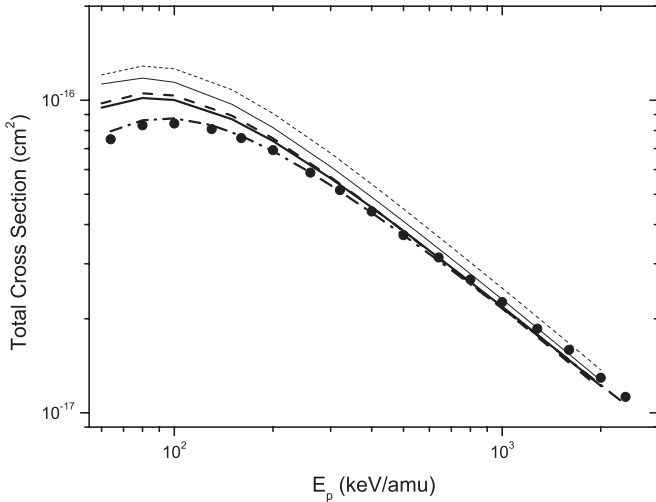
FIG. 3. Total cross section as a function of incident projectile energy, for He ionization by proton impact. Thick(thin) curves: 5Z(1Z) initial functions. Solid lines: prior approximation. Dashed lines: post approximation. Dash-dotted lines: numerical functions from OPM potential. Dots: experimental data from Shah and Gilbody [26].

In Fig. 3 we compare the TCSs with the experimental data [26]. This figure displays the post and prior approaches for the initial states and effective final charges described above. The cross sections evaluated with the 1Z initial state are larger than those obtained with the 5Z state over the whole range of projectile energies. The prior CDW-EIS version exhibits smaller values than the post version for both initial functions when the electron-target final state is represented by a Coulomb state. The post and prior formalisms give comparable results for the initial 5Z functions and converge to OPM results and experimental data for energies higher than 200 keV. The ionization energy associated with the 5Z function is higher than for the 1Z state and, therefore, allows for smaller cross sections, as shown in Fig. 3. The cross section evaluated with the 1Z function in the post version is larger than that given by the prior version over the whole energy range. This is a consequence of the sensibility of the post version to the final charge; a change in this charge could produce a better convergence. Evaluation of the TCS requires an integration on $v\,dE$ of the angular distributions, and the differences shown in Fig. 1 at high electron velocities become more significant. For the lower displayed energies the overestimation of the TCS is virtually due to the description of the atomic state and related to the ionization energy as stated before. The CDW-EIS method is in very good agreement with the experimental results in the case of H targets where exact atomic wave functions are available [1]. The analogous situation is presented here with the precise numerical OPM functions for the ground and continuum states of He. This approach is in good agreement with the experimental data over the entire projectile energy range considered. Above 500 keV the differences between the different approximations, except for the 1Z post, are quite small. Meanwhile, for energies higher than 200 keV the 5Z wave approach gives an excellent description with considerably less computational work than for the numerical approach.

III. ELECTRON EMISSION PROBABILITIES

The usual models employed for evaluation of multiple-ionization cross sections are the independent electron and the independent event models, which consider the process as a sequence of direct single ionizations produced by the projectile of each single electron. In the independent electron model the probability of direct ionization of N electrons is calculated by a binomial distribution of products of the single atomic ionization probabilities. These probabilities can be evaluated from the transition matrix defined in the former section, using a Fourier transform. A usual approximation assumes a symmetry in the azimuthal angle of the transferred momentum [11,14].

The transition matrix T_{fi} is a function of $\boldsymbol{k}_1$ and $\boldsymbol{K}_f$, but it can also be expressed as a function of the transferred momentum $\boldsymbol{Q} = \boldsymbol{K}_i - \boldsymbol{K}_f$. By energy conservation, the matrix element depends only on the transversal component $\boldsymbol{\eta}$ of $\boldsymbol{Q}$, in the plane perpendicular to the incident direction; that is, $\boldsymbol{\eta} \cdot \boldsymbol{v} = 0$. Then

$$\frac{d\sigma}{d\boldsymbol{k}_1 d\boldsymbol{\eta}} = (2\pi)^4 \frac{1}{v^2} |T_{fi}|^2. \tag{4}$$

A Fourier transform gives the scattering amplitude in terms of the impact parameter $\boldsymbol{\rho}$, which also lies in the plane perpendicular to the impact velocity:

$$A_{fi}(\boldsymbol{\rho},\boldsymbol{k}_1) = \frac{1}{2\pi} \int e^{-i\boldsymbol{\rho}\cdot\boldsymbol{\eta}} T_{fi}(\boldsymbol{\eta},\boldsymbol{k}_1)\, d\boldsymbol{\eta}, \tag{5}$$

$$T_{fi}(\boldsymbol{\eta},\boldsymbol{k}_1) = \frac{1}{2\pi} \int e^{i\boldsymbol{\rho}\cdot\boldsymbol{\eta}} A_{fi}(\boldsymbol{\rho},\boldsymbol{k}_1)\, d\boldsymbol{\rho}, \tag{6}$$

and

$$\frac{d\sigma}{d\boldsymbol{k}_1} = \frac{(2\pi)^4}{v^2} \int |A_{fi}(\boldsymbol{\rho},\boldsymbol{k}_1)|^2 d\boldsymbol{\rho}. \tag{7}$$

The use of $A_{fi}(\boldsymbol{\rho},\boldsymbol{k}_1)$ instead of $T_{fi}(\boldsymbol{\eta},\boldsymbol{k}_1)$ also allows for the introduction of the internuclear interaction, as shown below. Equation (5) is a double integral in η and the angle φ_η between $\boldsymbol{\eta}$ and a fixed axis in the plane orthogonal to $\boldsymbol{K}_i$. The direction of this fixed axis is generally chosen as the projection of $\boldsymbol{k}_1$ in that plane. The usual approximation is to assume $\varphi_\eta = 0$, meaning that $\boldsymbol{\eta}$ and $\boldsymbol{k}_1$ are in the same plane, and one integration is avoided in Eq. (5) [11,14]. With this axial symmetry the scattering amplitude can be written

$$A_{fi}^0(\boldsymbol{\rho}) = \int J_0(\eta\rho) T_{fi}(\eta,\varphi_\eta = 0)\, \eta\, d\eta.$$

This is denominated as a Bessel transform. The differences between these two amplitudes have been thoroughly discussed by Gulyás *et al.* [4]. As shown there, the single-electron-ionization TCSs evaluated from the amplitude $A_{fi}(\boldsymbol{\rho},\boldsymbol{k}_1)$ or $A_{fi}^0(\boldsymbol{\rho},\boldsymbol{k}_1)$ are identical, independent of the approximation used and whether or not the internuclear interaction is considered.

We can define two models of ionization probability for an ion impinging with impact parameter $\boldsymbol{\rho}$:

$$P(\boldsymbol{\rho}) = \int |A_{fi}(\boldsymbol{\rho},\boldsymbol{k}_1)|^2 d\boldsymbol{k}_1, \tag{8}$$

$$P^0(\boldsymbol{\rho}) = \int \left|A_{fi}^0(\boldsymbol{\rho},\boldsymbol{k}_1)\right|^2 d\boldsymbol{k}_1. \tag{9}$$
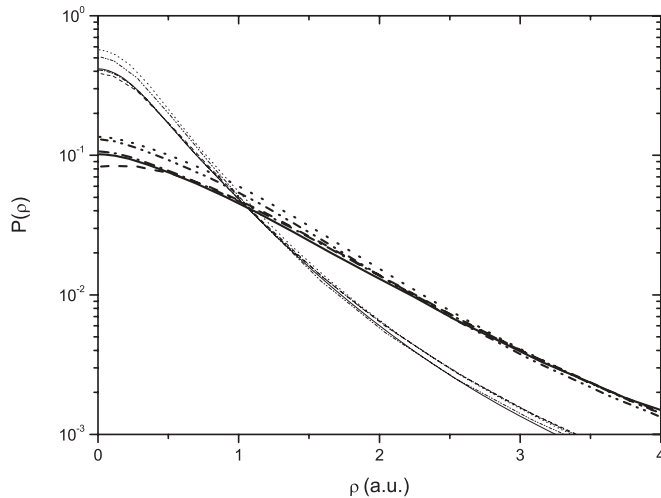
FIG. 4. Ionization probabilities as a function of the impact parameter for 500 keV proton impact. Thick(thin) curves: Fourier(J_0) transform. Solid lines: results obtained by applying numerical functions from an OPM potential. Dot-dashed lines: 5Z initial function under the post approximation. Dotted lines: 1Z initial function under the post approximation. Dashed line: 5Z initial function under the prior approximation. Dot-dot-dashed lines: 1Z initial function under the prior approximation.

FIG. 5. $\rho P(\rho)$ as a function of the impact parameter for 500 keV proton impact. Thick(thin) curves: Fourier(J_0) transform. Solid lines: results obtained by applying numerical functions from an OPM potential. Dot-dashed lines: 5Z initial function under the post approximation. Dotted lines: 1Z initial function under the post approximation. Dashed line: 5Z initial function under the prior approximation. Dot-dot-dashed lines: 1Z initial function under the prior approximation.

These two functions are shown in Fig. 4 for protons impinging on He atoms at 500 keV, evaluated with the prior and post versions of the CDW-EIS approximation, 1Z and 5Z initial states, and final Coulomb continuum electron-target state. They are contrasted with the case in which initial and final wave functions are evaluated with an OPM potential.

As shown in Fig. 4, all the probabilities resulting from the hypothesis of axial symmetry look similar, even for those derived from the OPM model. The same observation is valid for those derived with the full Fourier transform. For better comparison in Fig. 5 we display the functions $\rho P^0(\rho)$ and $\rho P(\rho)$, which are the integrands in the evaluation of the TCSs. We observe that the Bessel transform increases the probabilities at small impact parameters, and the Fourier transform concentrates at intermediate ones, in every case. The different initial waves with post or prior versions lead to quite different probabilities and conserve the relative distribution already shown for the TCSs in Fig. 3. Larger deviations are observed for the 1Z wave function cases. At large impact parameters, the $\rho P^0(\rho)$ probability falls more rapidly than the $\rho P(\rho)$. Similar behavior was observed for other collision energies.

The evaluation of multiple-ionization probabilities contains products of the single-ionization probabilities. This will increase the differences between the approximations, and the resulting multiple probabilities will be very sensitive to the chosen initial waves and CDW-EIS version. It is clear that the relative relation between the prior and the post approximations will be kept even in this case. For multiple ionization the cross section resulting from the Bessel transform will deviate strongly from the correct one obtained from the full Fourier transform, and the axial symmetry assumption will not be applicable.
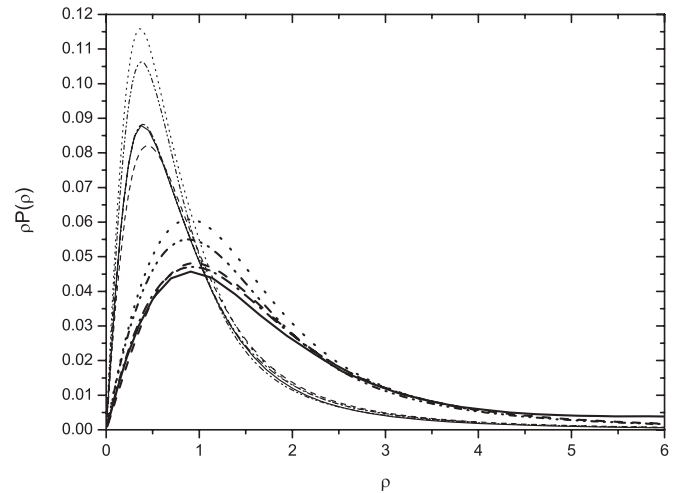
IV. INTERNUCLEAR INTERACTION

The internuclear interaction plays an important role in some particular features of the ionization differential cross sections. It can be neglected for the evaluation of cross sections that do not explicitly depend on the momentum transferred by the projectile in the collision, in particular, when an impact parameter method is used [15].

Recent experimental techniques allow simultaneous measurement of the momenta of the emitted electrons and the recoiling residual-target ion. This gives direct evidence of the momentum transferred by the projectile in the collision [18,27] and the internuclear interaction must be considered. The simplest way to introduce this interaction in a distorted wave method is to first evaluate $A_{fi}(\boldsymbol{\rho})$ without the N-N interaction and then define a new transition matrix with the N-N interaction by introducing a simple phase [28]:

$$T_{fi}^N(\boldsymbol{\eta}) = \frac{1}{2\pi} \int e^{-i\boldsymbol{\rho}\cdot\boldsymbol{\eta}} e^{i\delta(\boldsymbol{\rho})} A_{fi}(\boldsymbol{\rho}) \, d\boldsymbol{\rho}. \tag{10}$$

The ion-ion phase factor results from the contraction of an eikonal phase in the initial and final state. When the projectile-nucleus potential is purely Coulombic [1],

$$e^{i\delta(\boldsymbol{\rho})} = (v\rho)^{i\frac{2Z_P Z_{Tf}}{v}}, \tag{11}$$

where Z_{Tf} is the effective charge assumed for the residual ion, as above. This interionic potential model is denoted C1. Another model for He targets is to assume a projectile-screened core potential [4], giving

$$e^{i\delta(\boldsymbol{\rho})} = e^{\frac{i}{v_P}\{2Z_P \ln(v\rho)+2Z_P[K_0(2Z_{Tf}\rho)+Z_{Tf}\rho K(Z_{Tf}\rho)]\}}. \tag{12}$$

In this case we assumed $Z_{Tf} = 2$. We denote this interionic potential model C2.

Cross sections for single ionization of He atoms by proton impact, with the differential in the projectile scattering angle θ_P, were measured some years ago [29]. Using a high-resolution projectile energy-loss spectrometer, these angular distributions have been measured for particular values of the projectile energy loss ΔE for He targets [30]. Recently similar measurements were performed for H targets. [31].

From Eq. (3) we can evaluate the differential cross sections in the projectile scattering angle:

$$\frac{d\sigma}{d\Omega_{K_f}} = (2\pi)^4 \mu^2 \frac{K_f}{K_i} \int |T_{fi}^N|^2 d\boldsymbol{k}_1. \qquad (13)$$

The scattering amplitude is evaluated by a Fourier transform of the scattering matrix without internuclear interaction, as in Eq. (5). Then we introduce the internuclear interaction, as given by Eqs. (11) or (12). A further Fourier transform provides the scattering matrix that incorporates the internuclear interaction, and by applying Eq. (13) we obtain the respective cross sections.

In Fig. 6 we represent the differential cross sections in the projectile final scattering angle for 300 keV protons impinging on He atoms. We found that there are no noticeable differences between the post and the prior cross sections in most of the angular range displayed; deviations are observed at very small angles. In Sec. II we saw that the difference between the post and the prior formalisms is given by an electron–heavy-particle kinematics differential correlation term. In a binary collision of the projectile with a stationary electron, the maximum deviation of the projectile could be 0.545 mrad. Therefore larger deviations are produced by ion-ion interaction and have a slight dependence on the prior or post formalism used. To simplify Fig. 6, only one curve was drawn in each case. We represent the post CDW-EIS cross sections with 1Z and
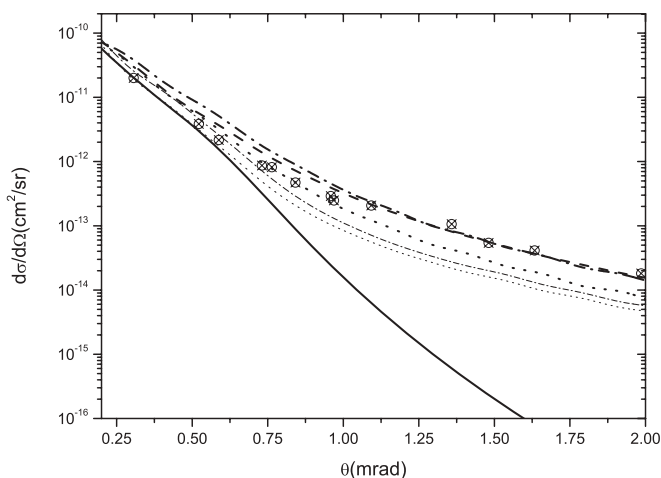

FIG. 7. Single-ifferential cross section for 500 keV protons impinging on He targets as a function of the projectile angular deviation. Thick(thin) curves: C1(C2) interionic potential model. Solid lines: calculations without *N-N* interaction with the OPM. Dashed line: numerical functions from OPM potential. Dash-dotted lines: 1Z initial state. Dotted lines: 5Z initial state. Dots: experimental data from Giese and Horsdal [29].
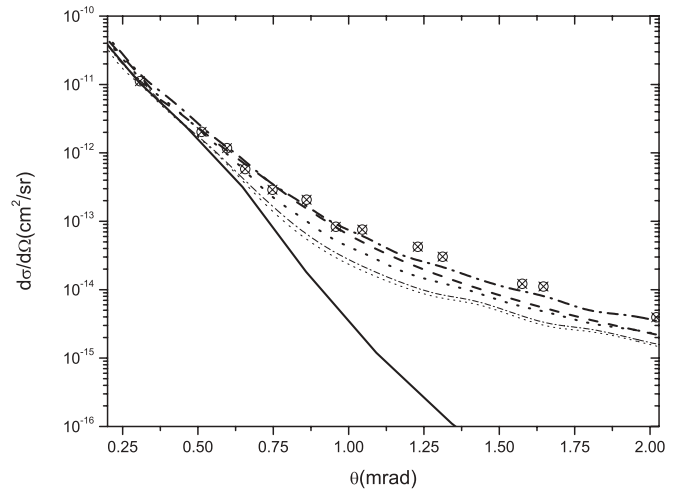
5Z initial states and final Coulomb continuum electron-target state, for the two alternative interionic potential models (C1 and C2). We also show the results when the initial and final wave functions are evaluated with an OPM potential.

The cross section resulting from the use of 1Z and 5Z waves shows differences at large projectile scattering angles; this feature can be inferred from Fig. 5, recalling that large deviation angles correspond to low impact parameters. The calculation of the CDW-EIS approximation without the *N-N* factor for this distribution drops to low values rapidly above the maximum binary collision angle.

The pure Coulombian *N-N* interaction (C1) provides a better fit to the experimental data than the screened potential model, which seems to be too weak in the large-angle region, where a head-on collision is probable. We observe differences between the angular distributions resulting from the 1Z and 5Z initial states with the Coulomb interionic model (C1), but they are smaller than the screened interaction (C2). The latter potential seems to underestimate the repulsion between the positive charges. Similar results are shown in Fig. 7 for a 500 keV collision, but the separation between the diverse approximations is smaller.

For high energies the low deviation angles correspond to distant collisions where the deflection of the proton is determined by the net effect of the interaction with the nucleus and target electrons. We see that in Fig. 7 the difference between the two models becomes smaller than in Fig. 6.

V. CONCLUSIONS

We calculated the CDW-EIS amplitude for the ionization of helium atoms by proton impact, using three types of initial wave functions, namely, hydrogenic 1Z, Clementi-Roetti 5Z, and OPM states. We used Coulomb functions with effective

FIG. 6. Single differential cross section for 300 keV proton impinging on He targets as a function of the projectile angular deviation. Thick (thin) curves: C1 (C2) interionic potential model. Solid lines: calculations without *N-N* interaction with OPM. Dashed line: numerical functions from OPM potential. Dash-dotted lines: 1Z initial state. Dotted lines: 5Z initial state. Dots: Experimental data from Giese and Horsdal [29].

charges and OPM functions, calculated from a Talman potential, for the final three-body state. Furthermore, we considered two perturbation Hamiltonians, the first associated with the initial state (prior approximation) and the second with the final state (post approximation).

The DDCS evaluated with the CDW-EIS method gives the soft and the ECC peaks but underestimates the DDCS for the interion velocity ridge and, consequently, provides a poor description of the asymmetry of the ECC peak, at intermediate energies. For high energies, the theoretical description of experimental values improves remarkably in any case, but the best results are obtained with the more precise OPM functions. We should note that with OPM functions there is no post-prior discrepancy.

The prior(post) CDW-EIS approach is very sensitive to the quality of the initial(final) states. In fact, the 5Z state provides an excellent description of the initial wave function and, applied to the prior version, gives cross sections equivalent to those obtained with the OPM functions, in agreement with data. As is well known, the CDW-EIS method improves at low values of the Sommerfeld parameter (Z_P/v_P).

The post-prior discrepancy is large in the TCS when using the 1Z initial wave function, even for very high energies. Furthermore, it decreases for 5Z initial states with final Coulomb states, but the precise OPM description is required for a good agreement with experiment at intermediate energies. However, the differences are not as large as those observed in the FDCS [8]. For impact energies higher than 200 keV the prior and post versions with 5Z and OPM functions match and agree with experiment. At any rate, the application of the 5Z function significantly reduces the computational time compared to that required when using the numerical OPM functions.

We evaluated the single-ionization probability as a function of the impact parameter by Fourier transforming the amplitude and, also, by introducing an axial symmetry for the final three-body system. The additional hypothesis of this axial symmetry leads to very high probabilities at low impact parameters, almost 5 times higher than the one resulting from the correct description; they decrease for increasing impact parameters. In both cases we observed a large spread of the probabilities evaluated in the post and prior versions with a 1Z initial wave. Instead, we observed small differences between the 5Z and the OPM results. The axial symmetry introduced saves one integration and gives the same TCS as when it is not assumed. This hypothesis leads to an incorrect description of the ionization process as a whole, focusing on the probabilities at low impact parameters and reducing the relevance of distant and medium-range collisions.

We also introduced two descriptions for the *N-N* interaction, and no relevant post-prior discrepancy was observed. The results showed that all approximations are larger than the experimental data for small projectile deviation angles, which are associated with large impact parameters (Figs. 6 and 7). At large angles, theoretical values obtained with OPM wave functions and the full Coulomb *N-N* interaction (C1) agree with the data. Without the *N-N* interaction the OPM description becomes very small for angles larger than the binary projectile-electron angle. The screened *N-N* interaction seems too weak and it is unable to describe the cross section at large projectile deviations. However, as the impact energy increases, the different approximations reduce their spread.

[1] D. S. Crothers and J. F. McCann, J. Phys B **16**, 3229 (1983).

[2] P. D. Fainstein, L. Gulyás, and A. Salin, J. Phys B **27**, L259 (1994).

[3] L. Gulyás, P. D. Fainstein, and A. Salin, J. Phys B **28**, 245 (1995).

[4] L. Gulyás, A. Igarashi, P. D. Fainstein, and T. Kirchner, J. Phys B **48**, 025202 (2008).

[5] G. Gasaneo, W. R. Cravero, M. D. Sanchez, and C. R. Garibotti, Phys. Rev. A **54**, 439 (1996).

[6] M. D. Sanchez, W. R. Cravero, and C. R. Garibotti, Phys. Rev. A **61**, 062709 (2000).

[7] M. F. Ciappina, W. R. Cravero, and C. R. Garibotti, J. Phys B **36**, 3775 (2003).

[8] M. F. Ciappina and W. R. Cravero, J. Phys B **39**, 1091 (2006).

[9] N. Stolterfoht, R. D. Dubois, and R. Rivarola, *Electron Emission in Heavy Ion-Atom Collisions* (Springer, Berlin, 1997).

[10] M. R. Fiori, G. Jalbert, C. E. Bielschowsky, and W. Cravero, Phys. Rev. A **64**, 012705 (2001).

[11] M. Fiori, A. Rocha, C. Bielschowsky, G. Jalbert, and C. R. Garibotti, J. Phys B **39**, 1751 (2006).

[12] J. M. Monti *et al.*, J. Phys B **43**, 205203 (2010).

[13] D. P. Marshall, C. Le Sech, and D. S. F. Crothers, J. Phys B **26**, L219 (1993).

[14] J. Bradley, R. Lee, M. McCartney, and D. S. Crothers, J. Phys B **37**, 3723 (2004).

[15] B. Bransden and M. R. McDowell, *Charge Exchange and the Theory of Ion-Atom Collisions* (Clarendon, Oxford, UK, 1992).

[16] R. Moshammer, Phys. Rev. Lett. **73**, 3371 (1994).

[17] J. Ullrich, R. Moshammer, A. Dorn, R. Dörner, L. Ph. H. Schmidt, and H Schmidt-Böcking, Rep. Prog. Phys. **66**, 1463 (2003).

[18] J. Ullrich and V. P. Shevelko, *Many-Particle Quantum Dynamics in Atomic and Molecular Fragmentation* (Springer, Berlin, 2003).

[19] J. Miraglia and C. R. Garibotti, Phys. Rev. **21**, 572 (1980).

[20] M. Foster, J. L. Peacher, M. Schulz, A. Hasan, and D. H. Madison, Phys. Rev. A **72**, 062708 (2005), and references therein.

[21] E. C. Clementi and C. Roetti, At. Data Nucl. Data Tables **14**, 177 (1974).

[22] J. D. Talman and W. F. Shadwick, Phys. Rev. A **14**, 36 (1975); J. D. Talman, Comput. Phys. Commun. **54**, 85 (1989).

[23] G. C. Bernardi, S. Suárez, P. D. Fainstein, C. R. Garibotti, W. Meckbach, and P. Focke, Phys. Rev. A **40**, 6863 (1989).

[24] D. H. Lee, P. Richard, T. J. M. Zouros, J. M. Sanders, J. L. Shinpaugh, and H. Hidmi, Phys. Rev. A **41**, 4816 (1990).

[25] L. Gulyás and P. D. Fainstein, J. Phys B **31**, 3297 (1998).

[26] M. B. Shah and H. B. Gilbody, J. Phys B **18**, 899 (1985); M. B. Shah, D. S. Elliott, and H. B. Gilbody, *ibid.* **18**, 4245 (1985).

[27] J. Ullrich *et al.*, J. Phys B **30**, 2917 (1997).

[28] M. R. McDowell and F. Coleman, *Introduction to the Theory of Ion Atom Collisions* (North-Holland, Amsterdam, 1970).

[29] J. P. Giese and E. Horsdal, Phys. Rev. Lett. **60**, 2018 (1988).

[30] T. Vajnai, A. D. Gaus, J. A. Brand, W. Htwe, D. H. Madison, R. E. Olson, J. L. Peacher, and M. Schulz, Phys. Rev. Lett. **74**, 3588 (1995).

[31] A. C. Laforge, K. N. Egodapitiya, J. S. Alexander, A. Hasan, M. F. Ciappina, M. A. Khakoo, and M. Schulz, Phys. Rev. Lett. **103**, 053201 (2009).